Journal of
Polymer Materials

Tech Science Press

Doi:10.32604/jpm.2025.059622

ARTICLE

Synergistic Effect of Piperazine Pyrophosphate (PAPP)/Melamine Polyphosphate (MPP)/ZnO Halogen-Free Flame Retardant System in PPC-P/PBAT Blends

Yuxin Zheng, Ke Xu, Baicheng Zhang, Shengxin Guan, Lin Xia and Zhaoge Huang*

Key Laboratory of Rubber-Plastics, Ministry of Education/Shandong Provincial Key Laboratory of Rubber-Plastics, School of Polymer Science and Engineering, Qingdao University of Science and Technology, Qingdao, 266042, China

*Corresponding Author: Zhaoge Huang. Email: hzg@qust.edu.cn

Received: 13 October 2024; Accepted: 30 December 2024; Published: 27 March 2025

ABSTRACT: In this manuscript, we conveniently prepared a series of polyester-polycarbonate copolymer (PPC-P)/polybutylene adipate terephthalate (PBAT) blends that exhibit both flame-retardant properties and toughness. Piperazine pyrophosphate (PAPP), melamine phosphate (MPP) and ZnO were used as synergistic flame retardants for PPC-P/PBAT blends. The effects of synergistic flame retardants on thermal stability, combustion behavior and flame retardancy of PPC-P/PBAT blends were investigated. The results showed that when the ratio of PAPP/MPP/ZnO was 18.4:9.2:2.4, the LOI of PPC-P/PBAT composite was 42.8%, and UL-94 reached V-0 level. The results of cone calorimetry showed that the mass loss rate (MLR), the peak value of the biggest smoke production rate (pSPR) and total smoke production (TSP) of the material decreased, and a continuously expanded carbon layer with a compact structure was formed after combustion. The carbon layer formed after surface combustion protects the material from decomposition over a long temperature range. In terms of mechanical properties, compared with the composites with only PAPP and MPP, PAPP/MPP/ZnO composites can improve the mechanical properties. After adding 2.4 wt% ZnO, the tensile strength and impact strength of the polymer increased to 34.2 MPa and 28.5 kJ/m^2, respectively. The results showed that the use of non-toxic, environmentally friendly, halogen-free flame retardants to enhance the flame retardant properties of biodegradable polymer composites is a promising direction in the future.

KEYWORDS: Polybutylene adipate terephthalate; polyester-polycarbonate copolymer; intumescent flame retardant; flame retardant properties; mechanical properties

1 Introduction

As industrialization accelerates globally, the synthesis of materials from petroleum resources releases substantial quantities of carbon dioxide (CO_2), drawing widespread concern for environmental warming. The quest for sustainable resources to create high-performance, eco-friendly materials has emerged as a pressing global challenge. In response to this issue, researchers have delved deeper into the direct utilization of CO_2 for the production of chemical monomers and polymers [1,2]. In response to the growing concern for environmental quality, there has been a shift towards the development of green and environmentally friendly materials, which has emerged as a new trend in recent years. At present, PLA is the most used degradable material, but it is made of starch raw materials made of renewable plant resources, and CO_2 cannot be recycled directly.

Fan et al. [3] successfully synthesized a polyester-polycarbonate copolymer (PPC-P) through bulk polymerization of carbon dioxide (CO_2), propylene oxide (PO), and phthalic anhydride (PA). Compared with other degradable plastics, CO_2 enters the reaction system as a raw material and replaces some organic matter to participate in the reaction, which can greatly reduce production costs in the future. The utilization of CO_2 in the synthesis process has played a significant role in addressing the issue of plastic pollution while also converting CO_2 into high-value products. PPC-P, however, is known to be a hard and brittle polymer material [4,5]. PPC-P exhibits low heat resistance and melting resistance during combustion, and its mechanical properties are suboptimal. To overcome these limitations, it is urgently required to modify PPC-P with ductile materials. One commonly used material for modifying brittle materials is polybutylene adipate terephthalate (PBAT), which provides high flexibility and ductility [6,7]. The utilization of PBAT for modification shows promising prospects for enhancing the performance of PPC-P [8–12].

The compatibility between PBAT and PPC-P can be effectively enhanced by incorporating a compatibilizer into the blends or by producing a compatibilizer through an *in-situ* reaction. Dicumyl peroxide (DCP), a frequently utilized peroxide cross-linking agent in polymer materials. Upon heating, DCP decomposes to generate alkoxy radicals. These radicals initiate chain transfer reactions leading to the formation of polymer radicals, which subsequently combine and terminate to produce a cross-linked network structure. The existence of this cross-linked network significantly enhances the material's mechanical properties and thermal stability. DCP is commonly used as a crosslinking agent for polyester materials, playing a crucial role in achieving *in-situ* compatibilization in composites [13]. It is mainly used as a polymer material initiator, crosslinking agent, curing agent and flame retardant additive. Studies have shown that the addition of DCP to polybutylene succinate (PBS) leads to branching and partial crosslinking reactions, significantly improving the mechanical properties and melt strength of PBS [14].

When traditional halogen flame retardants are used in flame retardant-modified polymer materials, they tend to release corrosive smoke and gases, posing a serious threat to the environment and human health [15,16]. In contrast, intumescent flame retardants (IFRs) offer several advantages, such as low smoke generation, non-toxicity, and anti-dripping properties [17–19]. These reagents undergo degradation upon heating, resulting in the formation of carbonized materials that create a physical barrier. During combustion, the internal materials are effectively isolated, preventing the transfer of oxygen and heat, while a carbon layer is formed on the surface of the polymer matrix, thereby achieving excellent flame retardancy [20–22]. In this experiment, we selected an intumescent flame retardant (IFR) system comprising Piperazine pyrophosphate (PAPP) and Melamine phosphate (MPP). This flame retardant combination was chosen due to the complementary chemical structures and properties of PAPP and MPP, allowing for synergistic interactions that enhance flame retardancy. Piperazine pyrophosphate contains piperazine groups, whereas Melamine phosphate contains melamine groups. These compounds can release substantial amounts of inert gases, such as nitrogen and carbon dioxide, at high temperatures. These gases form a protective layer during combustion, isolating oxygen and effectively inhibiting flame spread. Additionally, the decomposition of PAPP and MPP generates inorganic acids that can facilitate surface charring of the material, creating a dense carbon layer that further impedes heat and oxygen transfer. Thus, the IFR system composed of PAPP and MPP demonstrates exceptional flame retardant capabilities, significantly enhancing material fire safety. PAPP is a single-molecule intumescent flame retardant synthesized through the copolymerization of piperazine and phosphoric acid [23]. Its molecular structure contains an acid source, foaming agent, and carbonization agent. PAPP exhibits a high initial decomposition temperature and excellent carbonization ability. PAPP has been successfully utilized in many resins, including vinyl acetate copolymers [24], thermoplastic elastomers [25], and polyamide 66 [26]. MPP serves as both an acid source and a foaming agent. MPP not only catalyzes the formation of a protective carbon layer but also releases non-combustible gases, such as

NH_3. MPP has been successfully employed in polyamides and polyesters [27]. The combination of PAPP and MPP enhances the formation of a high-quality carbon layer. Chen et al. [28] used PAPP/MPP/TiO_2 as a flame retardant for thermoplastic elastomers (TPE). When 40 wt% PAPP/MPP/TiO_2 was added to TPE, the elastomer achieved a flammability rating of UL-94 V-0 and an LOI value of 37.8%, which was 116% higher than that of pure TPE. Furthermore, the thermal stability of the flame retardant material and its enhanced char yield were observed in the thermogravimetric (TG) tests conducted in both nitrogen and air atmospheres. These findings indicate a synergistic interaction between PAPP and MPP, which promotes the formation of high-quality carbon layers. Currently, polypropylene carbonate (PPC-P) is a novel degradable plastic, and there have been few studies investigating the flame retardancy of PAPP/MPP in PPC-P matrix. PPC-P materials have significant brittle defects, limiting their widespread practical use and making it challenging to directly incorporate them into production processes. To address this limitation, modifying PPC-P is typically necessary to enhance its adaptability and meet diverse application needs. One commonly used modification approach is blending PPC-P with other polymers to create alloy materials. For instance, the degradable resin PBAT can be blended with PPC-P to improve its brittleness and overall performance. However, alloy materials derived from PPC-P and PBAT often face issues with poor phase compatibility in applications, leading to phase interface separation [29–31]. This drawback compromises the material's overall performance and diminishes its practical utility.

To address this issue, this paper proposes an innovative modification strategy involving optimizing the two-phase interface separation of PPC-P/PBAT alloy materials by adding dicumyl peroxide (DCP). Simultaneously, to meet the dual requirements of environmental protection and material performance, this paper utilizes halogen-free flame retardants, specifically intumescent flame retardants (IFR), to fabricate PPC-P/PBAT alloy materials with exceptional mechanical and flame-retardant properties to align with market demands. The primary objective of this research was to investigate the impact of different proportions of the flame retardant system on the material properties and identify the optimal synergistic effects. This innovative flame-retardant PPC-P/PBAT material introduces new perspectives for creating flame-retardant 3D printing materials. With the growing focus on environmental conservation and the adoption of sustainable practices, PPC-P, as a biodegradable material, will play an increasingly crucial role in future industrial production and daily life.

2 Experimental

2.1 Materials

PPC-P, which was obtained from Shandong Lianxin Environmental Protection Technology Co., Ltd. (Shandong, China), has a glass transition temperature (T_g) of 46°C. PBAT, specifically the 0625 grade, was provided by Jinhui Zhaolong High-tech Co., Ltd. (Shanxi, China), and has a T_g of −29.8°C. DCP was sourced from Sinopec Shanghai Gaoqiao Petrochemical Co., Ltd. (Shanghai, China). PAPP was purchased from Shanghai Research Institute of Chemical Industry (Shanghai, China), while MPP was supplied by Minglang Plastics Co., Ltd. (Changzhou, China). ZnO was obtained from Shanghai McLean Biochemical Co., Ltd. (Shanghai, China).

2.2 Preparation of the Flame Retardant Composites

The plasticizing process of these composites is prepared in the torque rheometer mixer (RM-200C, Harbin Hapu Electric Technology Co., Ltd., Harbin, China) at a temperature of 145°C and a speed of 50 rpm. After 8 min of mixing, the mixture is compressed into a tablet using an open mill at a temperature of 50°C. Standard samples were prepared by preheating at 145°C for 7 min, followed by hot pressing at 145°C and a pressure of 10 MPa for 5 min. Finally, cold pressing was done at 25°C with a pressure of 10 MPa for 3 min

using a plate vulcanizing machine (XLB type) manufactured by Qingdao Yadong Rubber Machinery Co., Ltd. (Qingdao, China). The formula is shown in Table 1.

Table 1: Flame retardant PPC-P/PBAT material ratio

Samples	Components					
	PPC-P (wt%)	PBAT (wt%)	DCP (wt%)	PAPP (wt%)	MPP (wt%)	ZnO (wt%)
PPC-P	100	0	0	0	0	0
PBAT	0	100	0	0	0	0
PPC-P/PBAT	80	20	0	0	0	0
PPC-P/PBAT/DCP	80	20	0.05	0	0	0
PPC-P/PBAT/DCP/PAPP20	64	16	0.05	20	0	0
PPC-P/PBAT/DCP/PAPP25	60	15	0.05	25	0	0
PPC-P/PBAT/DCP/PAPP30	56	14	0.05	30	0	0
PPC-P/PBAT/DCP/PAPP35	52	13	0.05	35	0	0
PPC-P/PBAT/DCP/PAPP10/MPP20	56	14	0.05	10	20	0
PPC-P/PBAT/DCP/PAPP15/MPP15	56	14	0.05	15	15	0
PPC-P/PBAT/DCP/PAPP20/MPP10	56	14	0.05	20	10	0
PPC-P/PBAT/DCP/PAPP22.5/MPP7.5	56	14	0.05	22.5	7.5	0
PPC-P/PBAT/DCP/PAPP19.2/MPP9.6/ZnO1.2	56	14	0.05	18.8	9.4	1.8
PPC-P/PBAT/DCP/PAPP18.4/MPP9.2/ZnO2.4	56	14	0.05	18.4	9.2	2.4

2.3 Characterizations

2.3.1 Limiting Oxygen Index (LOI)

According to the ASTM D2863-2000 standard, the critical oxygen index test was conducted using the TTech-GBT2406-1 analyzer (manufactured by Testech Testing Instrument Technology Co., Ltd., Suzhou, China).

2.3.2 Vertical Combustion Performance (UL-94)

The vertical burning test was conducted using the CZF-3 horizontal and vertical combustion tester (Ningbo Huixin Instrument Technology Co., Ltd., Ningbo, China) in accordance with the American UL-94 test standard ASTM D3801. The sample size used for the test was 127.0 mm × 12.7 mm × 1.6 mm.

2.3.3 Thermogravimetric Analysis (TGA)

The TGA experiment was conducted using a thermogravimetric analyzer STA 8000 (PerkinElmer, Shelton, CT, USA). The test samples were heated from room temperature to 900°C at a heating rate of 10°C/min, and the test was conducted under a nitrogen atmosphere.

2.3.4 Cone Calorimeter Analysis (CONE)

The cone calorimeter (6810-YYV4, Suzhou Yangyi Walch Testing Technology Co., Ltd., Suzhou, China) was used to conduct tests in accordance with the ISO 5660 standard. The samples used had dimensions of 100 mm × 100 mm × 4 mm, and the heat flux was set at 35 kW/m^2. The main parameters measured or recorded included time to ignition (TTI), mass loss rate (MLR), smoke production rate (SPR), heat release rate (HRR), total smoke production (TSP), and residual mass after combustion.

2.3.5 Laser Spectrum Analysis

The laser spectrum confocal microscope (KC-X1000, Suzhou Kaimaishi Electronics Co., Ltd., Suzhou, China) was used for testing. The parameters were measured according to the ISO 25178 detection standard, with a scanning speed of 80 mm/s and a *Z*-axis resolution of 2 nm.

2.3.6 Scanning Electron Microscopy (SEM)

The residues collected from the cone calorimeter test were coated with a layer of gold and observed under a scanning electron microscope (Regulus 8100, Hitachi Ltd., Tokyo, Japan).

2.3.7 Mechanical Performance Test

According to the ISO 527-1 standard, the tensile strength test was conducted using a CMT4204 (Shenzhen Meister Co., Ltd., Shenzhen, China) universal testing machine. The test was performed at a speed of 10 mm/min. The unnotched impact strength was measured using a 2.75 J pendulum on the GT-7045-MDH cantilever beam impact tester (High-speed Rail Technology Co., Ltd., Taiwan, China).

2.3.8 Thermogravimetry-Infrared Spectroscopy (TG-IR)

Infrared spectroscopy (FTIR), using a Nicolet in 10 MX instrument by Thermo Scientific Co., Ltd. (Waltham, MA, USA), was utilized to analyze and characterize the molecular structure during carbon formation. A potassium bromide (KBr) disk was employed for detection, with a resolution of 128 cm^{-1}.

3 Results and Discussion

3.1 Flame Retardancy Behavior

The LOI and UL-94 test results for PPC-P/PBAT composites are presented in Table 2. In flammability combustion testing, the sample without any flame retardant did develop a carbon layer and burned continuously. This caused the combustion products to drip densely and ignite the cotton ball, resulting in a test failure. However, with the addition of 30 wt% PAPP, the UL-94 rating reached V-1 level. In this experiment, we observed that the sample failed to ignite the adjacent cotton wool during combustion. This phenomenon suggested that the fire droplets produced did not reach the ignition temperature of the cotton wool, preventing combustion. This indicated that the sample exhibits effective flame retardant properties, inhibiting flame spread and enhancing overall flame retardancy.

Table 2: LOI and vertical combustion results of PPC-P/PBAT and PPC-P/PBAT/IFR composites

Samples	t_1 (s)	t_2 (s)	Dripping	Ignition of Cotton	UL-94 Rating	LOI (%)
PPC-P	Burn-to-clamp	–	Yes	Yes	NR	19.6
PBAT	Burn-to-clamp	–	Yes	Yes	NR	24.3
PPC-P/PBAT	Burn-to-clamp	–	Yes	Yes	NR	21.5
PPC-P/PBAT/DCP	Burn-to-clamp	–	Yes	Yes	NR	22.1
PPC-P/PBAT/DCP/PAPP20	0	38	Yes	Yes	V-2	28
PPC-P/PBAT/DCP/PAPP25	0	25	Yes	Yes	V-2	29.5
PPC-P/PBAT/DCP/PAPP30	0	17	Yes	No	V-1	30.8
PPC-P/PBAT/DCP/PAPP35	0	4	No	No	V-0	33
PPC-P/PBAT/DCP/PAPP10/MPP20	0	0	No	No	V-0	31.6
PPC-P/PBAT/DCP/PAPP15/MPP15	0	0	No	No	V-0	34.2
PPC-P/PBAT/DCP/PAPP20/MPP10	0	0	No	No	V-0	36.6
PPC-P/PBAT/DCP/PAPP22.5/MPP7.5	0	0	No	No	V-0	36.5
PPC-P/PBAT/DCP/PAPP19.2/MPP9.6/ZnO1.2	0	0	No	No	V-0	41.2
PPC-P/PBAT/DCP/PAPP18.4/MPP9.2/ZnO2.4	0	0	No	No	V-0	42.8

Furthermore, by increasing the PAPP content to 35 wt%, the UL-94 rating improved to V-0 level. However, considering that the high content of flame retardants can lead to a decrease in the mechanical properties of the material, the content of UL-94 is used when the mutation occurs in order to reduce the negative impact of flame retardants as fillers. Considering all the properties, 30 wt% PAPP was chosen for subsequent experiments.

The LOI value for pure PPC-P is only 19.6%, indicating poor flame retardant performance. However, by incorporating PAPP/MPP in the composites, the LOI value increased, resulting in reduced flammability. When the ratio of PAPP/MPP is 2:1, the composite achieved an LOI value of 36.6%. By adding different amounts of ZnO on this basis, the LOI value further improved to over 41%. In the PPC-P/PBAT/DCP/IFR/ZnO system, the LOI value reached 42.8%, attributed to the decomposition of DCP produces isopropylphenoxy radical, which crosslinks with PPCP and PBAT while forming a cross-linked network structure induced by nano-ZnO [32]. These results demonstrate the synergistic effect between PAPP and MPP in the composite phase, while the incorporation of ZnO in the IFR system enhances the flame retardancy of PPC-P/PBAT/DCP/IFR composites.

3.2 TG Analysis Results

Thermogravimetric analysis (TGA) is commonly used to study the thermal degradation behavior of flame retardant materials, employing a small heat flux method [33]. Fig. 1 illustrates the mass loss and mass loss rate curves of PPC-P/PBAT composites under a nitrogen (N_2) atmosphere, while Table 3 provides corresponding data from these curves. $T_{1\%}$ represents the temperature at which decomposition initiates, T_{max} represents the temperature at which the maximum mass loss occurs, and $R_{800°C}$ refers to the mass ratio of the residue at 800°C. The addition of flame retardants lowers the decomposition temperature of the material. This is due to the decomposition of PAPP and MPP at lower temperatures, resulting in the formation of viscous substances such as phosphoric acid and $(HPO_3)_n$. These substances coat the surface of the matrix, acting as a barrier to prevent combustion.

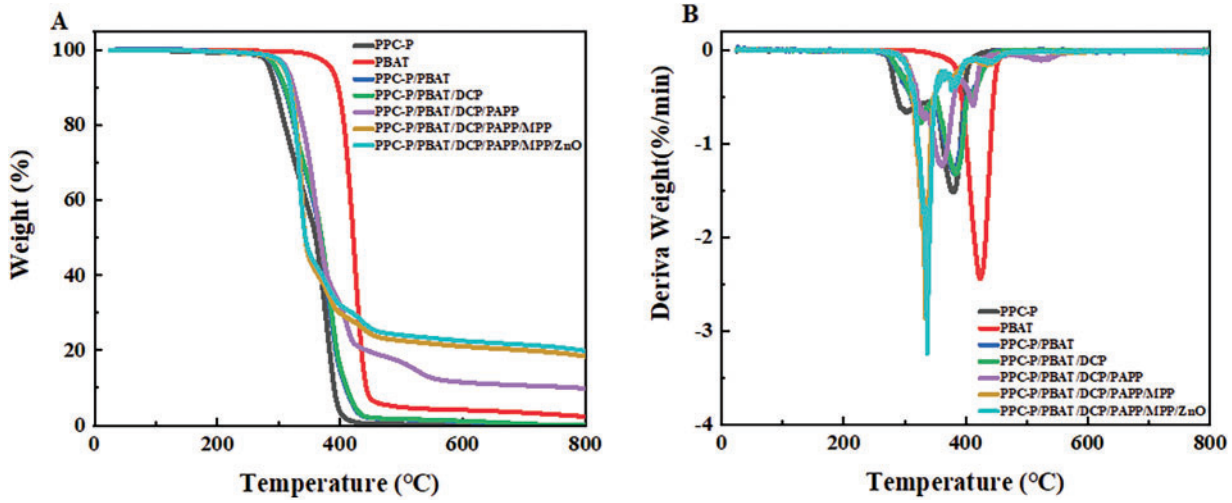

Figure 1: TG(A) and DTG(B) curves of PPC-P/PBAT and PPC-P/PBAT/IFR composites

Table 3: Thermogravimetric data of PPC-P, PBAT and composites in N_2 atmosphere

Samples	$T_{1\%}$ (°C)	T_{max} (°C)	$R_{800°C}$ (wt%)
PPC-P	186	377	0.12
PBAT	253	413	1.21
PPC-P/PBAT	189	373	0.08
PPC-P/PBAT/DCP	192	378	0.02
PPC-P/PBAT/DCP/PAPP	137	351	9.71
PPC-P/PBAT/DCP/PAPP/MPP	98	335	18.09
PPC-P/PBAT/DCP/PAPP/MPP/ZnO	100	329	18.71

In the absence of any flame retardant additives, pure PPC-P started decomposing at approximately 186°C, while pure PBAT began decomposing at around 253°C. Both materials underwent complete decomposition at 800°C, leaving behind very little residue in the PPC-P/PBAT polymer system. The addition of DCP has no effect on the thermal properties of the material. However, when the system was modified with an intumescent flame retardant (IFR), the residual carbon content reached 18.09%. Furthermore, the addition of ZnO increased the residual carbon content to 19.56%. The residual carbon content of the system still increases, even taking into account the fact that some ZnO added will not cause thermal gratings. These results indicate the effectiveness of the IFR/ZnO system in enhancing thermal stability and delaying the degradation of the material.

From the DTG curve (Fig. 1B), it is evident that the intumescent flame retardant (IFR) system follows a one-step decomposition behavior, occurring at temperatures between 350°C and 430°C. This can be attributed to the decomposition of PAPP, a single-component IFR, which generates piperazine, $[PON]_m$, and non-combustible gas [28]. The resulting phosphoric acid and its derivatives accelerate the carbonization reaction. Additionally, the curve after adding MPP has a peak value at 336.9°C because $(HPO3)_n$ is generated [27], which serves as an acid source, while piperazine acts as a carbon source. The esterification reaction between the acid source and the carbon source leads to the dehydration of the carbon source, resulting in the formation of a molten carbon layer [34]. This molten carbon layer acts as a barrier to hinder the combustion behavior of the material, making it less prone to decomposition during continued combustion.

3.3 Cone Calorimetry

3.3.1 Cone Calorimetry Results

Fig. 2 illustrates the mass loss rate, smoke generation, and heat release rate of the material. The cone calorimeter test results provide an evaluation of the material's combustion characteristics and enable predictions of its behavior in real fire scenarios. It is observed that the TTI (Time to Ignition) value of PPC-P/PBAT/DCP/IFR/ZnO is lower than that of PPC-P/PBAT/DCP/IFR. This could be attributed to factors such as a decrease in specific heat capacity, a decrease in ignition temperature, or changes in the decomposition process caused by the addition of ZnO [35].

From Table 4, it can be observed that the mass residue rate of the IFR system is above 35%. Specifically, when 20 wt% PAPP and 10 wt% MPP are added, the mass residue rate can even reach 40.1%. In the initial phase of combustion, both the IFR and IFR/ZnO flame retardant systems played a significant role. Approximately 130 s after combustion began, these systems started to take effect by releasing non-flammable gases and forming a carbon layer on the material surface. This layer isolated oxygen and prevented heat transfer, effectively slowing down combustion and suppressing flame spread. The IFR and IFR/ZnO flame

retardant systems played a crucial role in enhancing material combustion safety and flame retardancy. As depicted in Fig. 2A, the addition of ZnO to the IFR system results in a relatively flat MLR (Mass Loss Rate) curve for the material. However, as the ratio of ZnO continues to increase, there is a slight increase in MLR during the main combustion stage (first 200 s). This can be attributed to the reaction between ZnO and the degradation products of PAPP, leading to the formation of gas phase products, which in turn increases the mass loss.

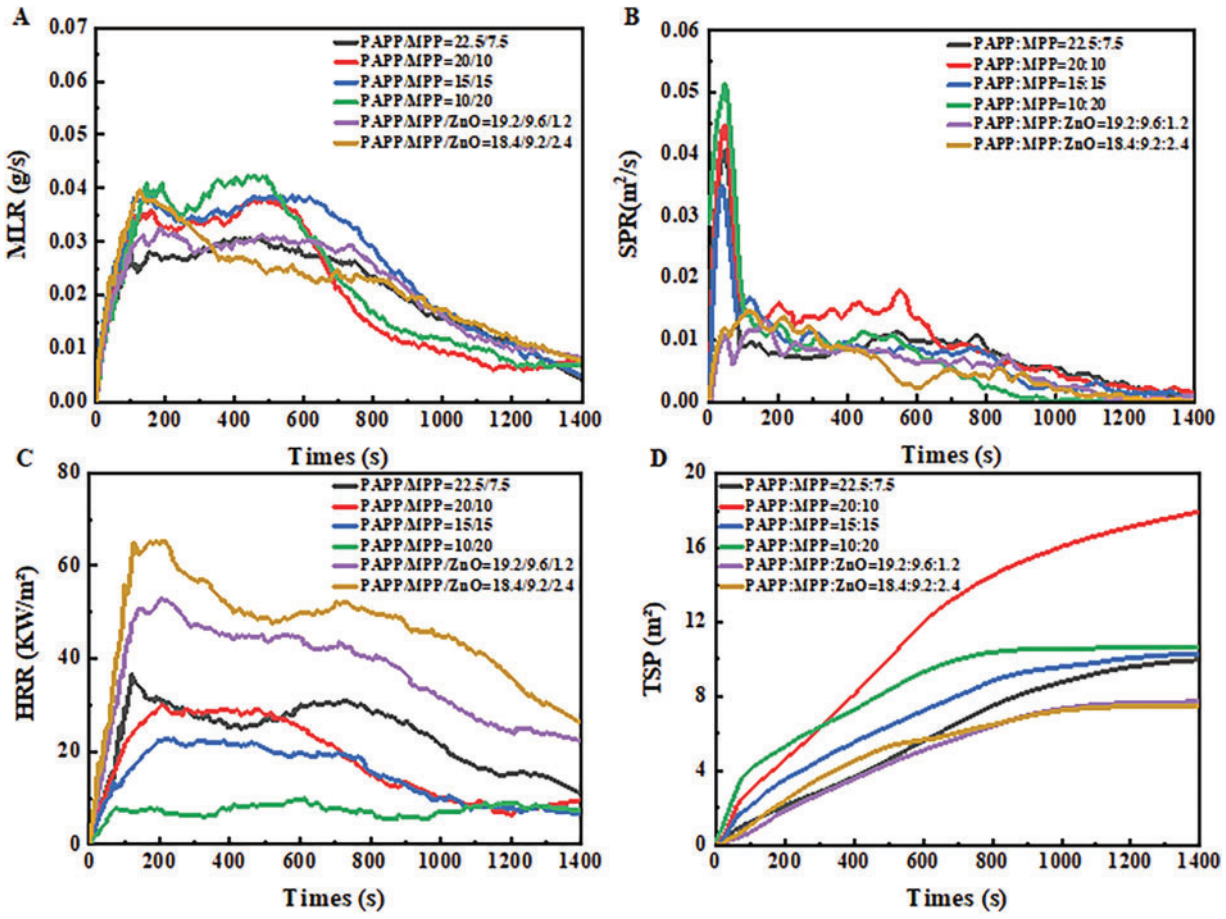

Figure 2: Curves of material mass loss rate (MLR) (A), smoke release rate (SPR) (B), heat release rate (HRR) (C), and total smoke release rate (TSP) (D) of PPC-P/PBAT/IFR composites during cone calorimeter test

Table 4: Combustion parameters of PPC-P/PBAT/IFR composites in cone calorimeter test

Samples	TTI (s)	Pk-HRR (kw/m²)	Pk-SPR (m²/s)	TSP (m²)	Final mass (wt%)
PPC-P/PBAT/DCP/PAPP10/MPP20	50 ± 1.3	9.9 ± 0.9	0.051 ± 0.003	10.6 ± 0.8	37.2 ± 2.3
PPC-P/PBAT/DCP/PAPP15/MPP15	43 ± 0.8	22.7 ± 2.0	0.035 ± 0.007	10.3 ± 0.4	35.4 ± 2.7
PPC-P/PBAT/DCP/PAPP20/MPP10	41 ± 1.7	30.1 ± 1.4	0.045 ± 0.011	18.0 ± 1.2	40.1 ± 1.6
PPC-P/PBAT/DCP/PAPP22.5/MPP7.5	46 ± 2.1	36.8 ± 1.8	0.041 ± 0.002	10.0 ± 0.3	37.8 ± 3.0
PPC-P/PBAT/DCP/PAPP19.2/MPP9.6/ZnO1.2	35 ± 1.1	52.7 ± 1.0	0.013 ± 0.009	7.7 ± 1.0	39.4 ± 2.6
PPC-P/PBAT/DCP/PAPP18.4/MPP9.2/ZnO2.4	28 ± 1.3	65.5 ± 2.3	0.015 ± 0.004	7.5 ± 1.5	42.7 ± 1.9

The smoke production rate (SPR) is an important parameter for quantifying the amount of flue gas generated. As shown in Fig. 2B,D, the SPR and TSP (Total Smoke Production) curves of PPC-P/PBAT/DCP/IFR composites are presented, respectively. The IFR system exhibits a peak at around 60 s during the main combustion stage, which is significantly reduced after the addition of ZnO. By adding 2.4 wt% ZnO, it was observed that the SPR decreased to 0.015 m^2/s and the TSP decreased to 7.5 m^2, effectively slowing down smoke release. This reduction can be attributed to the strong interaction between the carbon residue and the material facilitated by ZnO. The significant decrease in smoke release indicates that PPC-P/PBAT/IFR/ZnO effectively lowers both flame and smoke hazards.

3.3.2 Surface Morphology Analysis

To further investigate the flame retardant mechanism of the PAPP/MPP system and ZnO in PPC-P/PBAT, the surface morphology of the samples after cone calorimeter testing was analyzed. Fig. 3 presents the cross-sectional view of the residual carbon layer following the cone calorimetry test. The morphology of the expanded coke layer of PAPP20/MPP10 is more representative (Fig. 3C), indicating a higher degree of expansion compared to the remaining PAPP/MPP system. Relying solely on PAPP for intumescent flame retardation may result in inadequate phosphorus and carbon content. Therefore, MPP is required in the flame retardant system to serve as a phosphorus and carbon source for ensuring the flame retardant effect. The optimal ratio is crucial for flame retardant performance. Only by accurately controlling the PAPP to MPP ratio can the phosphorus and carbon content be optimized, thus achieving the best flame retardant effect. Incorrect ratios may lead to subpar flame retardant performance or complete failure. Therefore, in practical applications, it is essential to determine the most suitable ratio through experiments and optimization to guarantee the efficiency and reliability of the flame retardant system. When zooming in on the internal part of the carbon layer, it is evident that the carbon layer structure is not uniform. The expansion degree of the inner carbon layer is too low, which may be due to the insufficient air source caused by the poor ratio of the blowing agent.

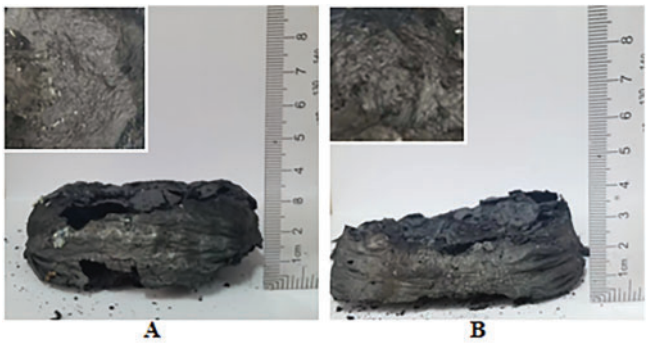

Figure 3: (Continued)

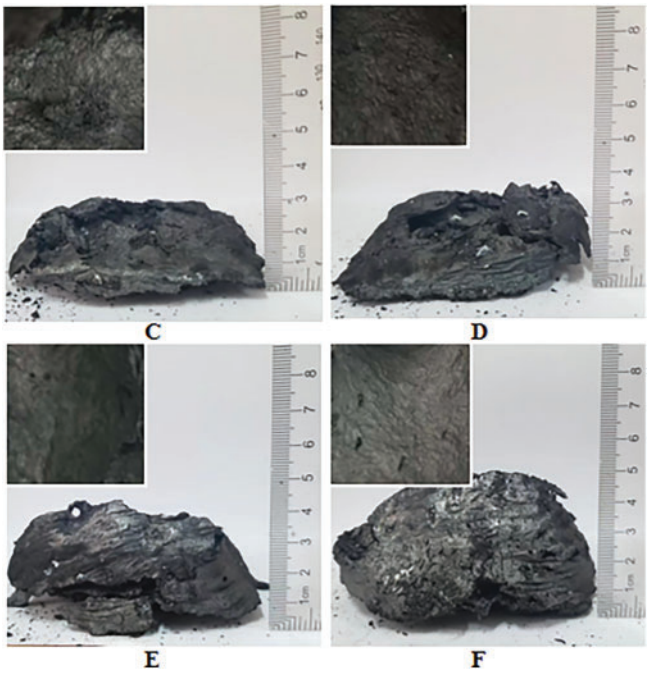

Figure 3: Residual image after cone calorimetric combustion (A) PAPP10/MPP20, (B) PAPP15/MPP15, (C) PAPP20/MPP10, (D) PAPP22.5/MPP7.5, (E) PAPP18.8/MPP9.4/ZnO1.8, (F) PAPP18.4/MPP9.2/ZnO2.4

In the case of the IFR/ZnO system (Fig. 3E,F), a continuous expanded carbon layer with dense, expanded, and thermally stable properties is formed after combustion. This expanded carbon layer is larger and more complete compared to other systems. Table 2 shows that PPC-P/PBAT/DCP/IFR/ZnO exhibits a higher char yield than PPC-P/PBAT/DCP/IFR. These findings indicate that the IFR/ZnO flame retardant system promotes the formation of more carbon residues and enhances the completeness of the carbon layer, thereby enhancing the protective effect.

3.3.3 Laser Spectroscopic Microanalysis

The laser spectrum analysis measurement module utilizes spectral confocal technology, which is combined with a feedback-controlled XY scanning module and a three-dimensional imaging algorithm to capture detailed surface structures. This technology is advantageous in avoiding data loss and edge distortion in areas with high slopes, thanks to the excellent angular characteristics inherent in spectral confocal technology. Fig. 4 illustrates the residue images obtained from the cone calorimeter test under the magnification of 330 times using a laser microscope. There were numerous small cracks on the surface of the residue in Fig. 4A–F. Fig. 4C highlighted that the addition of PAPP20/MPP10 enhanced the consolidation of the char layer, resulting in a dense and uniform char layer. This characteristic contributed to an excellent flame retardant effect in the condensed phase. Furthermore, when comparing Fig. 4C,F, it was evident that the inclusion of PAPP18.4/MPP9.2/ZnO2.4 resulted in a denser carbon layer with a honeycomb pore structure. The larger pores disappear, leaving only a few dense pores for gas exchange. These dense pores effectively delay the combustion process.

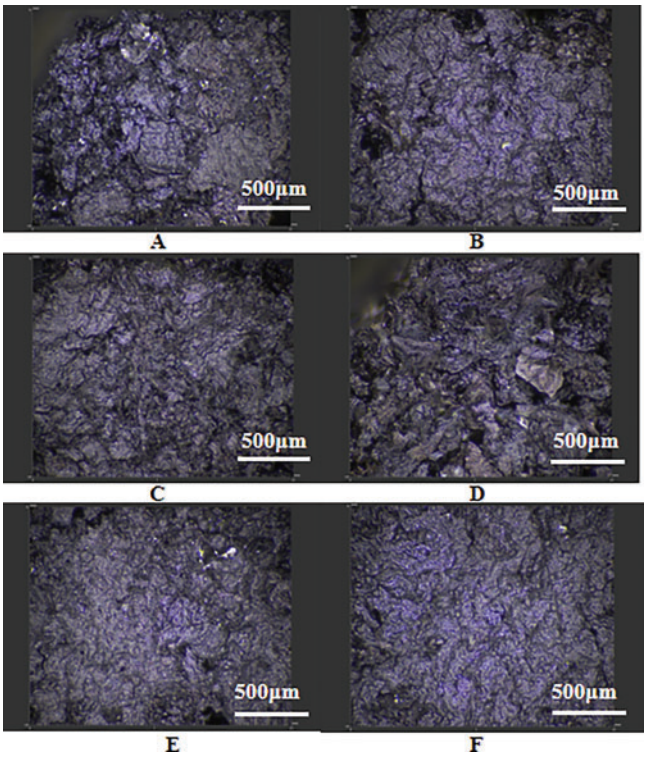

Figure 4: Carbon residue image under laser microscope (A) PAPP10/MPP20, (B) PAPP15/MPP15, (C) PAPP20/MPP10, (D) PAPP22.5/MPP7.5, (E) PAPP18.8/MPP9.4/ZnO1.8, (F) PAPP18.4/MPP9.2/ZnO2.4

3.3.4 Micromorphology Analysis

MPP and PAPP are known to release non-combustible gases, such as CO_2 and NH_3, at high temperatures. These gases help dilute the concentration of combustible gases on the material surface [36], thereby causing the residual carbon to become loose due to gas volatilization. Fig. 5 presents a comparison of different proportions of the PAPP/MPP flame retardant system. It can be observed that PAPP20/MPP10 (Fig. 5C) exhibits a lamellar structure under SEM observation, with a smooth surface and no apparent voids. In other proportions, the composite has an irregular structure, rough surface and obvious holes, which confirms the conclusion of the laser microscope in Fig. 4.

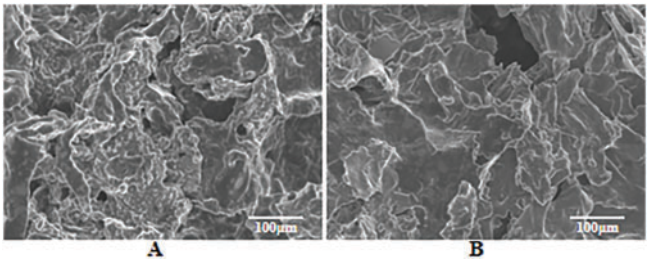

Figure 5: (Continued)

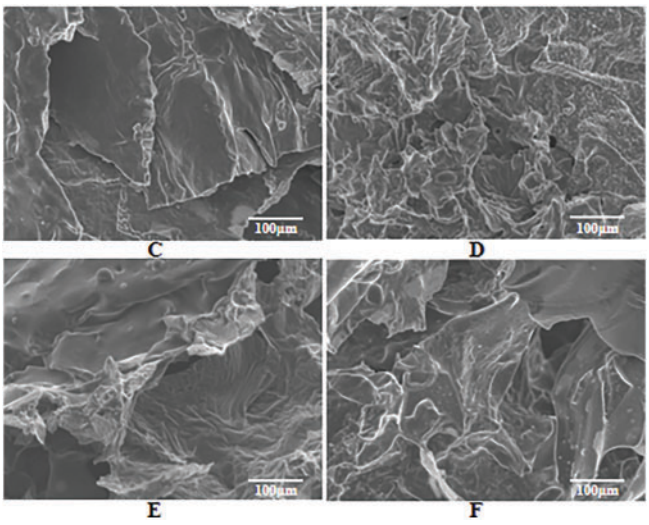

Figure 5: SEM images of residue after cone calorimetric combustion (A) PAPP10/MPP20, (B) PAPP15/MPP15, (C) PAPP20/MPP10, (D) PAPP22.5/MPP7.5, (E) PAPP18.8/MPP9.4/ZnO1.8, (F) PAPP18.4/MPP9.2/ZnO2.4

After incorporating ZnO into the PAPP/MPP flame retardant system (Fig. 5E,F), it becomes evident that there are minimal cracks or voids present. This addition enables the rapid formation of a dense honeycomb-like cross-linked carbonized carbon layer. The resulting intumescent carbon layer is both dense and lightweight, effectively inhibiting heat transfer and the supply of combustible gas during the combustion of the composite material [37].

3.4 Mechanical Properties

The mechanical properties of materials are the main basis for selecting various uses, which determines their application in different scenarios. In order to further evaluate the impact of the intumescent flame retardant (IFR) on PPC-P/PBAT/DCP composites, the mechanical properties of the composites were tested and compared. The specific data, including tensile strength and impact strength, can be found in Table 5.

Table 5: Effect of IFR content on tensile property and impact strength of PPCP/PBAT/DCP composite

Samples	Tensile strength (MPa)	Imapct strength (kJ/m^2)
PPC-P/PBAT/DCP	41.3 ± 3.6	38.4 ± 1.1
PPC-P/PBAT/DCP/PAPP20	33.2 ± 3.0	26.2 ± 1.6
PPC-P/PBAT/DCP/PAPP25	29.4 ± 1.5	25.8 ± 1.0
PPC-P/PBAT/DCP/PAPP30	28.2 ± 2.8	24.3 ± 0.7
PPC-P/PBAT/DCP/PAPP35	26.8 ± 1.9	21.8 ± 1.3
PPC-P/PBAT/DCP/PAPP10/MPP20	27.2 ± 2.3	24.2 ± 2.1
PPC-P/PBAT/DCP/PAPP15/MPP15	29.1 ± 3.7	24.7 ± 2.3
PPC-P/PBAT/DCP/PAPP20/MPP10	27.2 ± 2.0	24.5 ± 1.4
PPC-P/PBAT/DCP/PAPP22.5/MPP7.5	28.8 ± 2.5	24.8 ± 1.1
PPCP/PBAT/DCP/PAPP19.2/MPP9.6/ZnO1.2	33.4 ± 2.6	27.7 ± 1.9
PPCP/PBAT/DCP/PAPP18.4/MPP9.2/ZnO2.4	34.2 ± 3.3	28.5 ± 2.0

The initial tensile strength and impact strength of the PPC-P/PBAT/DCP composites were measured to be 41.3 MPa and 38.4 kJ/m^2, respectively. However, upon the addition of the intumescent flame retardant (IFR), the mechanical properties of the composites showed a decrease. This can be attributed to the island structure formed by the flame retardant, which reduces the interfacial force between the phases and subsequently affects the overall mechanical performance. To address this issue, a different amount (1.2 and 2.4 wt%) of ZnO was incorporated into the PAPP/MPP system. As a result, the tensile strength improved by 18% and 21%, while the impact strength increased by 14% and 17%, respectively. This can be explained by the strong interaction formed between the carbon residue and the material, thanks to the reaction facilitated by the presence of ZnO [38].

3.5 Infrared Spectrum

The gas decomposition products during carbon formation were analyzed using TG-FTIR. Fig. 6 displays the gas evolution spectrum of the flame retardant composites containing PAPP18.4/MPP9.2/ZnO2.4, as well as the infrared spectrum of the residual carbon layer after cone calorimetry. Table 6 presents the characteristic peak positions of the released gases during combustion. The main gas components detected are hydrocarbons, CO, and CO_2, which predominantly originate from the decomposition of PPC-P. Fig. 6A demonstrates that the initial decomposition temperature of PPC-P ranges between 250°C and 350°C. However, with the addition of the flame retardant, the decomposition of the material is effectively inhibited.

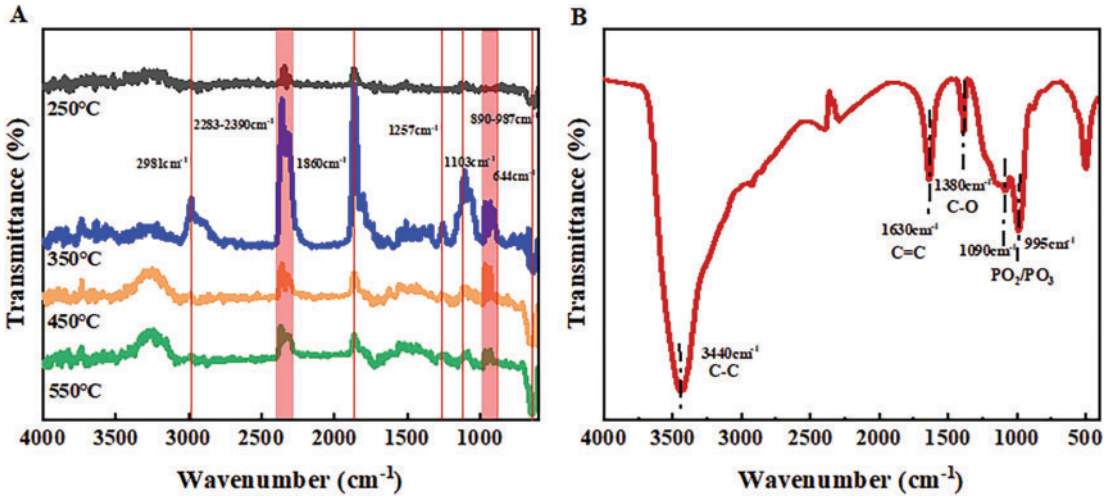

Figure 6: Infrared spectra of gases escaping at different temperatures (A) and residual infrared spectra after cone calorimetry (B)

Table 6: Characteristic peak positions of gases emitted during combustion of flame retardant materials

Evolved gases	FTIR/cm^{-1}
CO_2	2358, 2310, 664
CO	1860
NH_3	966, 929
Hydrocarbons	2981, 988
Phosphorous compounds	1103, 1257

The flame retardant composites release NH_3 at 350°C, primarily generated by the decomposition of MPP, its confirms the peak of the DTG curve at 336.9°C. NH_3 is a non-combustible gas that facilitates the expansion of the carbon layer and acts as a diluting agent for combustible gases in the gas phase [39]. Furthermore, the pyrolysis products at 350°C exhibit strong absorption peaks of phosphorus-containing compounds such as P-O (1103 cm^{-1}) and P=O (1257 cm^{-1}). These compounds further dilute the inert gas of combustible gases and can function as flame retardants in the gas phase.

Fig. 6B demonstrates that the condensed phase after cone calorimetry predominantly comprises phosphorus compounds (PO_2/PO_3 at 1090 and 995 cm^{-1}), while ammonia compounds primarily exist in the gas phase, contributing to flame retardancy. These observations can be attributed to the decreased release of organic volatiles during the combustion of PPC-P and the increased formation of carbon residues observed in the cone calorimeter test and TG test of PPC-P/PBAT/DCP/IFR composites.

3.6 Reaction Mechanism

Fig. 7 depicts the combustion reaction mechanism and specific synergistic flame retardant mechanism of PPC-P/PBAT/DCP/IFR/ZnO composites. During the initial stage of combustion, PAPP and MPP decompose, leading to an esterification reaction between the decomposition products. This promotes the rapid formation of a dense, expandable, and heat-resistant carbon layer. The formation of this char layer occurs prior to the rapid decomposition of the PPC-P/PBAT material. Consequently, it acts as a protective barrier, preventing further decomposition over a wide temperature range [40]. This carbon layer plays a crucial role in enhancing flame retardancy and thermal stability.

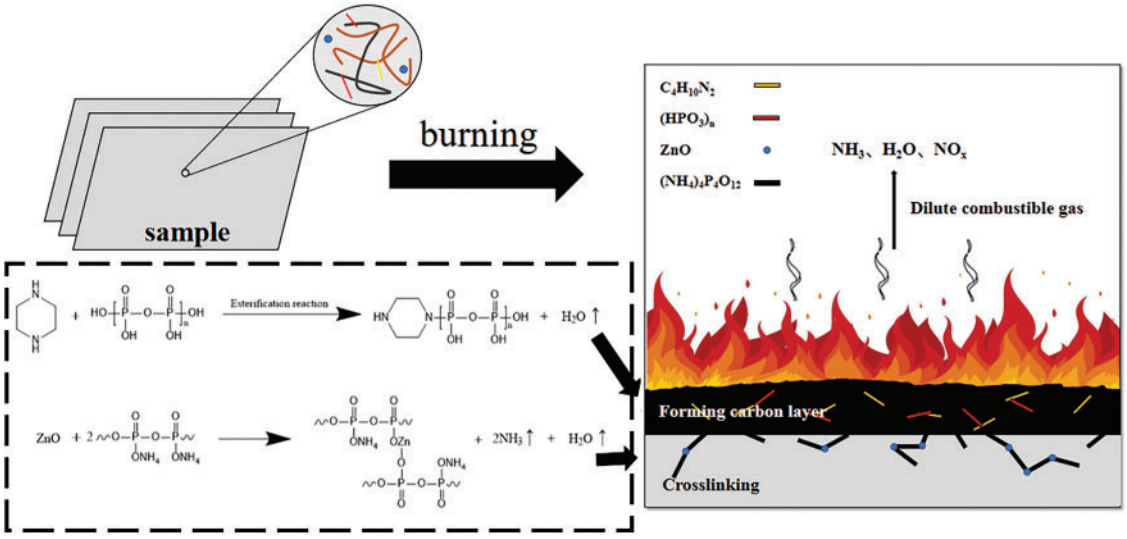

Figure 7: Combustion mechanism diagram of PAPP/MPP/ZnO flame retardant system

During the combustion process, the flame retardant mechanism of IFR operates in both the condensed phase and the gas phase. The non-combustible gas produced by the decomposition of PAPP and MPP impedes gas phase combustion and reduces the concentration of combustible substances in the gas phase. Moreover, the dense carbon layer formed after combustion acts as a barrier, inhibiting the polymer's combustion [41]. Furthermore, with the addition of ZnO, it reacts with the degradation products of PAPP to create a cross-linked network and releases non-combustible gases like NH_3 and H_2O. Non-combustible gases can dilute the concentration of combustible gases. This leads to the formation of a robust

carbon layer that is resistant to collapse, thereby significantly improving the flame retardant properties of PPC-P/PBAT/DCP composites.

4 Conclusion

The aim of this study was to investigate the effects of incorporating halogen-free flame retardants, specifically PAPP/MPP and ZnO, into PPCP/PBAT composites through melt blending. The research focused on evaluating the impact of flame retardant modification on the thermal stability, combustion behavior, and flame retardancy of composites. The incorporation of MPP and ZnO in PPC-P/PBAT/DCP/IFR/ZnO composites resulted in improved mechanical properties. Specifically, the tensile strength increased to 34.2 MPa, while the impact strength reached 28.5 kJ/m^2. Overall, these findings indicated that the inclusion of IFR/ZnO in the composite led to improved mechanical properties and increased resistance to combustion. Through blending PBAT with PPC-P, we have not only addressed material brittleness but also enhanced its flame-retardant properties. This innovative flame-retardant PPC-P/PBAT material introduces new perspectives for creating flame-retardant 3D printing materials. With the growing focus on environmental conservation and the adoption of sustainable practices, PPC-P, as a biodegradable material, will play an increasingly crucial role in future industrial production and daily life.

Acknowledgement: None.

Funding Statement: Financial support from National Natural Science Foundation of China (Grant No. 22075298), National Key R&D Program of China (2022YFD2301204) is gratefully acknowledged.

Author Contributions: The authors confirm contribution to the paper as follows: study conception and design: Yuxin Zheng, Ke Xu; data collection: Baicheng Zhang; analysis and interpretation of results: Shengxin Guan; draft manuscript preparation: Lin Xia, Zhaoge Huang. All authors reviewed the results and approved the final version of the manuscript.

Availability of Data and Materials: The data that support the findings of this study are available from the corresponding author upon reasonable request.

Ethics Approval: Not applicable.

Conflicts of Interest: The authors declare no conflicts of interest to report regarding the present study.

References

1. Muthuraj R, Mekonnen T. Recent progress in carbon dioxide (CO_2) as feedstock for sustainable materials development: co-polymers and polymer blends. Polymer. 2018;145:348–73. doi:10.1016/j.polymer.2018.04.078.
2. Xu Y, Lin L, Xiao M, Wang S, Smith AT, Sun L, et al. Synthesis and properties of CO_2-based plastics: environmentally-friendly, energy-saving and biomedical polymeric materials. Prog Polym Sci. 2018;80:163–82. doi:10.1016/j.progpolymsci.2018.01.006.
3. Fan C, Liang J, Ye S, Zhu Y, Wang S, Meng Y, et al. Study of the synthesis of CO_2/propylene epoxide/phthalic anhydride terpolymers with different sequence structures and their properties. Chin J Polym Sci. 2022;53:497–504. doi:10.11777/j.issn1000-3304.2021.21402.
4. Liang J, Wang S, Wu C, Wang S, Han D, Huang S, et al. A new biodegradable CO_2-based poly(ester-co-carbonate): molecular chain building up with crosslinkable domain. J CO_2 Util. 2023;69(37):102403. doi:10.1016/j.jcou.2023.102403.
5. Wang W, Ye S, Liang J, Fan C, Zhu Y, Wang S, et al. Architecting branch structure in terpolymer of CO_2, propylene oxide and phthalic anhydride: an enhancement in thermal and mechanical performances. Chin J Polym Sci. 2022;40(5):462–8. doi:10.1007/s10118-022-2686-4.

6. Gigante V, Canesi I, Cinelli P, Coltelli MB, Lazzeri A. Rubber toughening of polylactic acid (PLA) with poly(butylene adipate-co-terephthalate) (PBAT): mechanical properties, fracture mechanics and analysis of ductile-to-brittle behavior while varying temperature and test speed. Polymers. 2019;115(1):125–37. doi:10.1016/j.eurpolymj.2019.03.015.
7. Fei ZX, Sun J, Cui C, Yin C, Zhan R, Shi LY, et al. Highly enhanced mechanical strength and toughness of biodegradable PBAT plastics through a biobased multiple hydrogen bonding strategy. Macromolecules. 2024;57(15):7043–51. doi:10.1021/acs.macromol.4c01153.
8. Mohammadi M, Heuzey MC, Carreau PJ, Taguet A. Morphological and rheological properties of PLA, PBAT, and PLA/PBAT blend nanocomposites containing CNCs. Nanomater. 2021;11:857. doi:10.3390/nano11040857.
9. Sousa FM, Costa ARM, Reul LTA, Cavalcanti FB, Carvalho LH, Almeida TG, et al. Rheological and thermal characterization of PCL/PBAT blends. Polym Bull. 2019;76(3):1573–93. doi:10.1007/s00289-018-2428-5.
10. Botta L, Titone V, Teresi R, Scarlata MC, Re GL, Mantia FPL, et al. Biocomposite PBAT/lignin blown films with enhanced photo-stability. Int J Biol Macromol. 2022;217:161–70. doi:10.1016/j.ijbiomac.2022.07.048.
11. Su S, Duhme M, Kopitzky R. Uncompatibilized PBAT/PLA blends: manufacturability, miscibility and properties. Materials. 2020;13(21):4897. doi:10.3390/ma13214897.
12. Sun J, Huang A, Luo S, Shi M, Song J, Luo H. Effect of chain extender on morphologies and properties of PBAT/PLA composites. J Thermoplastic Compos Mater. 2023;36(3):1175–86. doi:10.1177/08927057211051415.
13. Muthuraj R, Misra M, Mohanty AK. Reactive compatibilization and performance evaluation of miscanthus biofiber reinforced poly(hydroxybutyrate-co-hydroxyvalerate) biocomposites. J Appl Polym Sci. 2017;134(21):44860. doi:10.1002/app.44860.
14. Ma P, Ma Z, Dong W, Zhang Y, Lemstra PJ. Structure/property relationships of partially crosslinked poly(butylene succinate). Macromol Mater Eng. 2013;298(8):910–8. doi:10.1002/mame.201200209.
15. Hu X, Yang H, Jiang Y, He H, Liu H, Huang H, et al. Facile synthesis of a novel transparent hyperbranched phosphorous/nitrogen-containing flame retardant and its application in reducing the fire hazard of epoxy resin. J Hazard Mater. 2019;379:120793. doi:10.1016/j.jhazmat.2019.120793.
16. Ai L, Chen S, Yang L, Liu P. Synergistic flame retardant effect of organic boron flame retardant and aluminum hydroxide on polyethylene. Fibers Polym. 2021;22(2):354–65. doi:10.1007/s12221-021-9385-6.
17. Wang J, Wang L, Xiao A. Recent research progress on the flame-retardant mechanism of halogen-free flame retardant polypropylene. Polym Plast Technol Eng. 2009;48:297–302. doi:10.1080/03602550802675645.
18. Lalegani Dezaki M, Branfoot C, Baxendale J, Bodaghi M. Bio-based gradient composites for 3D/4D printing with enhanced mechanical, shape memory, and flame-retardant properties. Macromol Mater Eng. 2024;27:562. doi:10.1002/mame.202400276.
19. Zhou Y, He W, Wu Y, Xu D, Chen X, He M, et al. Influence of thermo-oxidative aging on flame retardancy, thermal stability, and mechanical properties of long glass fiber-reinforced polypropylene composites filled with organic montmorillonite and intumescent flame retardant. J Fire Sci. 2019;37(2):176–89. doi:10.1177/0734904119833014.
20. Huang Z, Li S, Tsai L, Jiang T, Ma N, Tsai F. Flame retardant polypropylene with a single molecule intumescent flame retardant based on chitosan. Mater Today Commun. 2022;33(8):104689. doi:10.1016/j.mtcomm.2022.104689.
21. Zhao T, Wu W, Hu H, Rui Z, Zhang X, Li J. The piperazine pyrophosphate intumescent flame retardant of polypropylene composites prepared by selective laser sintering. Polym Compos. 2023;44(1):305–17. doi:10.1002/pc.27046.
22. Wu Z, Wang Q, Fan Q, Cai Y, Zhao Y. Synergistic effect of Nano-ZnO and intumescent flame retardant on flame retardancy of polypropylene/ethylene-propylene-diene monomer composites using elongational flow field. Polym Compos. 2019;40(7):2819–33. doi:10.1002/pc.25091.
23. Xu M, Xia S, Liu C, Li B. Preparation of poly(phosphoric acid piperazine) and its application as an effective flame retardant for epoxy resin. Polymers. 2018;36(5):655–64. doi:10.1007/s10118-018-2036-8.
24. Sun H, Chen K, Liu Y, Wang Q. Improving flame retardant and smoke suppression function of ethylene vinyl acetate by combining the piperazine pyrophosphate, expandable graphite and melamine phosphate. Eur Polym J. 2023;194(12):112148. doi:10.1016/j.eurpolymj.2023.112148.

25. Zhu M, Jia P, Sun P, Yu F, Yang G, Hu Y, et al. Core-shell structure antioxidant microencapsulated piperazine pyrophosphate towards improving service performance and fire safety of styrenic thermoplastic elastomer. Composites. 2023;174:107732. doi:10.1016/j.compositesa.2023.107732.
26. Tang W, Cao Y, Qian L, Chen Y, Qiu Y, Xu B, et al. Synergistic charring flame-retardant behavior of polyimide and melamine polyphosphate in glass fiber-reinforced polyamide 66. Polymers. 2019;11(11):1851. doi:10.3390/polym11111851.
27. Zhang T, Zhang Q, Yu Y, Chen T, Song N, Chen Z, et al. Effects of melamine polyphosphate on explosion characteristics and thermal pyrolysis behavior of polyamide 66 dust. J Loss Prev Process Ind. 2022;78(6):104820. doi:10.1016/j.jlp.2022.104820.
28. Chen T, Xiao X, Wang J, Guo N. Fire, thermal and mechanical properties of TPE composites with systems containing piperazine pyrophosphate (PAPP), melamine phosphate (MPP) and titanium dioxide (TiO_2). Plastics, Rubber Compos. 2019;48(4):149–59. doi:10.1080/14658011.2019.1582200.
29. Deng J, Yue S, Xiao M, Huang S, Wang S, Han D, et al. High-gas-barrier and biodegradable PPC-P/PBAT composite films coated by poly(vinyl alcohol)/borax complexes. Surfaces. 2024;7(3):517–28. doi:10.3390/surfaces7030034.
30. Yang J, Song X, Chen D, Liu Y, Wang Y, Shi J. The improvement of flame retardancy and compatibility of PBAT/PLLA via a hybrid polyurethane. Int J Biol Macromol. 2024;273:133057. doi:10.1016/j.ijbiomac.2024.133057.
31. Gao FX, Cai Y, Liu SJ, Wang XH. High-performance biodegradable PBAT/PPC composite film through reactive compatibilizer. Chin J Polym Sci. 2023;41(7):1051–8. doi:10.1007/s10118-023-2900-z.
32. Chen Y, Wu X, Li M, Qian L, Zhou H. Construction of crosslinking network structures by adding ZnO and ADR in intumescent flame retardant PLA composites. Polymers Adv Technol. 2022;33(1):198–211. doi:10.1002/pat.5505.
33. Cervantes-Uc JM, Cauich-Rodríguez JV, Vázquez-Torres H, Licea-Claveríe A. TGA/FTIR study on thermal degradation of polymethacrylates containing carboxylic groups. Polym Degrad Stab. 2006;91(12):3312–21. doi:10.1016/j.polymdegradstab.2006.06.005.
34. Sut A, Metzsch-Zilligen E, Großhauser M, Pfaendner R, Schartel B. Synergy between melamine cyanurate, melamine polyphosphate and aluminum diethylphosphinate in flame retarded thermoplastic polyurethane. Polym Test. 2019;74(4):196–204. doi:10.1016/j.polymertesting.2019.01.001.
35. Lizundia E, Penayo MC, Guinault A, Vilas JL, Domenek S. Impact of ZnO nanoparticle morphology on relaxation and transport properties of PLA nanocomposites. Polym Test. 2019;75(2):175–84. doi:10.1016/j.compositesb.2019.02.043.
36. Chen X, Wang W, Jiao C. A recycled environmental friendly flame retardant by modifying para-aramid fiber with phosphorus acid for thermoplastic polyurethane elastomer. J Hazard Mater. 2017;331:257–64. doi:10.1016/j.jhazmat.2017.02.011.
37. Yang P, Wu H, Yang F, Yang J, Wang R, Zhu Z. A novel self-assembled graphene-based flame retardant: synthesis and flame retardant performance in PLA. Polymers. 2021;13(23):4216. doi:10.3390/polym13234216.
38. Chen X, Ma C, Jiao C. Enhancement of flame-retardant performance of thermoplastic polyurethane with the incorporation of aluminum hypophosphite and iron-graphene. Polym Degrad Stab. 2016;129:275–85. doi:10.1016/j.polymdegradstab.2016.04.017.
39. Zhang L, Chai W, Li W, Semple K, Yin N, Zhang W, et al. Intumescent-grafted bamboo charcoal: a natural nontoxic fireretardant filler for polylactic acid (PLA) composites. ACS Omega. 2021;6(41):26990–7006. doi:10.1021/acsomega.1c03393.
40. Yuan Z, Wen H, Liu Y, Wang Q. Synergistic effect between piperazine pyrophosphate and melamine polyphosphate in flame retarded glass fiber reinforced polypropylene. Polym Degrad Stab. 2021;184(11):109477. doi:10.1016/j.polymdegradstab.2020.109477.
41. Yargici Kovanci C, Nofar M, Ghanbari A. Synergistic enhancement of flame retardancy behavior of glass-fiber reinforced polylactide composites through using phosphorus-based flame retardants and chain modifiers. Polymers. 2022;14(23):5324. doi:10.3390/polym14235324.